R.G. Cherkez, P.P. Fenyak, D.D. Demyanyuk

Institute of Thermoelectricity of the NAS and MES of Ukraine,
1, Nauky Str., Chernivtsi, 58029, Ukraine

COMPUTER SIMULATION OF PERMEABLE COOLING THERMOELEMENT

The results of computer research on a 3 D model of permeable thermoelement for cooling liquid and gas flows are presented. The physical model and design of permeable thermoelement is described, its mathematical description is given. A method for thermoelement calculation based on the Comsol Multiphysics package of applied computer programs has been created. The energy characteristics of thermoelement of Bi-Te-Se-Sb based materials have been calculated as a function of heat carrier pumping rate and supply voltage. The optimal values of hear carrier rate at thermoelement inlet whereby the values of cooling capacity and coefficient of performance will be maximum have been determined. Comparison of the energy characteristics of liquid and air cooling has shown their 30 to 50 % better values on water cooling.
Key words: permeable thermoelement, simulation, thermodynamic characteristics, semiconductors, cooling capacity, coefficient of performance.

Introduction

The widest application of thermoelectric power converters is based on the use of a thermocouple element [1, 2] whose energy conversion efficiency is determined by the figure of merit Z of used materials. Therefore, a search for materials with a maximum figure of merit value becomes the main challenge of thermoelectric material science. However, despite the active research pursued in this direction, there has been no essential figure of merit growth in recent 20 to 30 years [3, 4]. The maximum values of the dimensionless figure of merit parameter of industrial thermoelectric materials remain at a level of 1 to 1.2. So, to improve the figure of merit, one should use new, non-traditional approaches which consist in the use of unconventional variants of physical models of a thermoelement which is the main component of thermoelectric power converter.

One of them is the use of thermoelements with a developed internal heat exchange surface, i.e. permeable thermoelements. In such thermoelements, heat exchange with the source of heat and heat sink occurs not only on the junctions, but also in the bulk of the leg. Already the first theoretical [5] and experimental [6] investigations of thermoelements for cooling gas flows demonstrated their good prospects. They indicate the possibility of energy conversion efficiency improvement by a factor of 1.3 to 1.4.

However, such investigations were performed for a single-dimensional model that does not describe accurately enough the conjugate processes of heat exchange in solid-heat carrier system. Therefore, it is necessary to create and study a more real 3 D model of permeable thermoelement which is the objective of this work.

Physical model and its mathematical description

A physical model of permeable thermoelement where heat exchange between the source of heat and heat sink takes place not only through connecting plates, but also in the bulk of the leg, is given in Fig. 1. It

includes *n-* and *p*-type legs 1 made of materials based on *Bi-Te-Se-Sb* which together with openings in connecting plates 3 form a system of channels for pumping heat carrier, namely water. The model takes into account the presence of transient layer 2 due to a combination of connecting plates with thermo-element legs that has the properties of a solder. The legs material is homogeneous and isotropic with known temperature dependences of electric conductivity $\sigma(T)$, the Seebeck coefficient $\alpha(T)$, thermal conductivity $\kappa(T)$. The thermoelectric medium takes into account the bulk Thomson and Joule-Lenz effects and the near-contact Peltier effect. The temperature of heat carrier at thermoelement inlet was assumed equal to hot junction temperature.
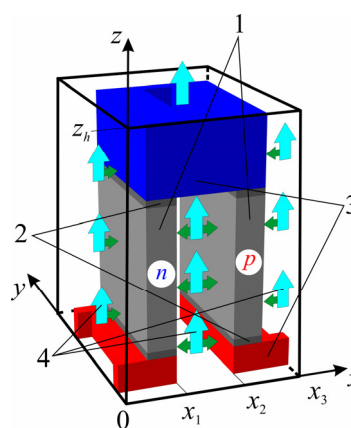

Fig. 1. Physical model of permeable thermoelement: 1 are n- and p-type legs; 2 is transient layer possessing the properties of a solder; 3 are connecting legs; 4 is heat carrier.

Heat exchange on the lateral surface of legs 1, connecting plates 3 and transient layer 2 that are in thermal contact with heat carrier 4 is described by the Newton-Richmann law:

$$q_0 = \alpha_T(t - T), \tag{1}$$

where α_T is heat exchange coefficient, T is thermoelement temperature, t is heat carrier temperature.

A system of equations describing the distribution of temperature and potential in thermoelectric medium is described by the fundamental laws of conservation of energy and current carriers [7]:

$$\nabla \vec{W} = 0, \tag{2}$$

$$\nabla \vec{i} = 0, \tag{3}$$

where $\vec{W} = \vec{q} + U\vec{i}$ is energy flux density.

Using the generalized Fourier's and Ohm's laws for the thermoelectric medium

$$\vec{q} = -\kappa \nabla T + \alpha \vec{i} T, \tag{4}$$

$$\vec{i} = -\sigma(\nabla U + \alpha \nabla T), \tag{5}$$

where U is potential, κ is thermal conductivity, α is the Seebeck coefficient, σ is electric conductivity, one can obtain a system of differential equations to find the distributions of temperatures and potentials:

$$\left. \begin{array}{l} \nabla \kappa \nabla T + \dfrac{i^2}{\sigma} - T\vec{i}\nabla\alpha = 0; \\ \nabla(-\sigma(\nabla U + \alpha \nabla T)) = 0. \end{array} \right\} \tag{6}$$

The Navier-Stokes equation system and the continuity equation are used to describe heat carrier motion along a channel, and thermal conductivity equation is used to describe temperature distribution in heat carrier.

The Navier-Stokes equation and the continuity equation can be written as [8]:

$$\left. \begin{array}{l} \rho \dfrac{d\vec{\vartheta}}{dt} = \rho\vec{F} - \nabla P + \mu\nabla^2\vec{\vartheta} + \dfrac{1}{3}\mu\nabla(div\vec{\vartheta}), \\ div\, \rho\vec{\vartheta} = 0. \end{array} \right\} \tag{7}$$

The left side of the first equation (7) is the inertia force. The first term on the right side of this equation describes mass (volumetric) force, the second term – surface pressure forces (normal stresses), and the last two terms – tangential components of surface forces (internal friction forces).

Heat exchange in liquid is described by thermal conductivity equation [9]:

$$\rho C_p \left(\frac{\partial t}{\partial \tau} + (\vec{\vartheta}\nabla)t \right) = -(\nabla \vec{q}) + \sum_{i,j} \Lambda_{ij} S_{ij} - \frac{t}{\rho} \frac{\partial \rho}{\partial t}\bigg|_P \left(\frac{\partial \rho}{\partial t} + (\vec{\vartheta}\nabla)P \right) + Q, \tag{8}$$

where ρ is liquid density, C_p is liquid specific heat, t is liquid temperature, $\vec{\vartheta}$ is liquid rate vector, $\vec{q}$ is heat flux density vector, P is pressure, Λ_{ij} is viscous stress tensor, $\vec{S}_{ij}$ is deformation rate tensor, Q are internal heat sources.

Of greatest practical interest is the problem of calculation of thermoelement energy characteristics in steady-state operating mode. In this case, time derivatives in (7) and (8) are set to zero. In the approximation of small influence of mass forces and insufficient liquid heating due to internal friction, its compression, as well as liquid heating at the cost of internal heat sources will be ignored in view of their small contribution as compared to thermoelectric thermal effects. In such approximations, the system of Navier-Stokes continuity and thermal conductivity equations will be written as:

$$\left. \begin{aligned} &-\nabla P + \mu \nabla^2 \vec{\vartheta} + \frac{1}{3}\mu \nabla (div\vec{\vartheta}) = 0, \\ &div\, \rho \vec{\vartheta} = 0, \\ &\rho C_p (\vec{\vartheta}\nabla)t + \nabla q = 0. \end{aligned} \right\} \tag{9}$$

The boundary conditions for this problem (Fig. 1), are given below:
– for thermoelectric medium

$$T\big|_{z=0} = 300\text{K}, \quad U\big|_{z=0} = 0, \quad U\big|_{x=x_3} = U_0, \quad q\big|_{S_b} = \alpha_T (t - T), \quad U\big|_{S_b} = 0, \tag{10}$$

– for heat carrier

$$\vartheta\big|_{z=0} = \vartheta_0, \quad P\big|_{z=z_h} = 0, \quad \vartheta\big|_{S_b} = 0, \quad t\big|_{z=0} = 300\text{K}, \quad q\big|_{S_b} = \alpha_T (T - t), \tag{11}$$

where ϑ_0 is heat carrier initial rate, U_0 is given potential value, S_b is thermoelement lateral surface.

Realization of the formulated problem in the Comsol Multiphysics package of applied computer programs

To perform the calculation, the Comsol Multiphysics package of applied computer programs was selected [10]. The general view of the coefficient form of equation in partial derivatives is as follows:

$$e_a \frac{\partial^2 \vec{u}}{\partial t^2} + d_a \frac{\partial \vec{u}}{\partial t} + \nabla(-c\nabla\vec{u} - \alpha\vec{u} + \gamma) + \beta\nabla u + a\vec{u} = f. \tag{12}$$

This equation is used for the thermoelectric medium and reduced to the form $\nabla(-c\nabla\vec{u}) = 0$. For this purpose, e_a, d_a, α, γ, β, a are set to zero, and the value c is written as a matrix:

$$c = \begin{pmatrix} \kappa + \alpha^2 \sigma T + \sigma U \alpha & \alpha T \sigma + \sigma U \\ \alpha \sigma & \sigma \end{pmatrix}. \tag{13}$$

In this case, vector $\vec{u}$ has also the form of a matrix:

$$\vec{u} = \begin{pmatrix} T \\ U \end{pmatrix}. \tag{14}$$

To describe liquid motion and heat exchange, the Comsol Multiphysics-Non-Isothermal Flow is used [11]. The module includes the Navier-Stokes equation system, the continuity equation and liquid heat transfer equation in the steady-state mode.

The electric current value was calculated through the integral according to sectional area S_V:

$$I = \iint\limits_{S_V} I_n \mathrm{d}S_V, \tag{15}$$

where $I_n = n_x I_x + n_y I_y + n_z I_z$ is electric current density vector. The values I_x, I_y, I_z, were determined by the relations:

$$I_x = -\sigma \frac{\partial U}{\partial x} - \sigma\alpha \frac{\partial T}{\partial x}, \tag{16}$$

$$I_y = -\sigma \frac{\partial U}{\partial y} - \sigma\alpha \frac{\partial T}{\partial y}, \tag{17}$$

$$I_z = -\sigma \frac{\partial U}{\partial z} - \sigma\alpha \frac{\partial T}{\partial z}. \tag{18}$$

Heat carrier flow rate was determined by integration of rate υ with respect to channel sectional area at liquid outlet S_{V1}:

$$G = \iint\limits_{S_{V1}} \vartheta \mathrm{d}S_{V1}. \tag{19}$$

The thermoelement electric power $W = I \cdot U$, cooling capacity was determined through heat carrier flow rate as $Q_c = G C_p \Delta t$, coefficient of performance $\varepsilon = Q_c / W$.

Results of computer research on the energy characteristics of liquid and air permeable thermoelement of materials based on *Bi-Te-Se-Sb*

The calculation was performed for materials based on *Bi-Te-Se-Sb*. Functional temperature dependences of material parameters, namely the Seebeck coefficient α, thermal conductivity κ and electric conductivity σ were obtained by the least squares method from their experimental data.

Simulation of permeable thermoelement was done for the following basic design (Fig. 2): height $h = 10$ mm, length $b = 10$ mm, width $a = 2$ mm. The dimensions of the lower connecting plates – height $j = 2$ mm, length $b = 10$ mm, width $k = 4$ mm; upper connecting plates – height $d = 5$ mm, length $c = 10$ mm, width $f = 8$ mm. Connecting material is copper. Connecting plates have cuts for heat carrier

Fig. 2. Design of permeable thermoelement.

pumping of length $n = 8$ mm, width $m = 2$ mm, located in the plate centre. These cuts together with legs form a system of channels for heat carrier pumping. The design takes into account the presence of transient solder layer of thickness $l = 0.5$ mm.
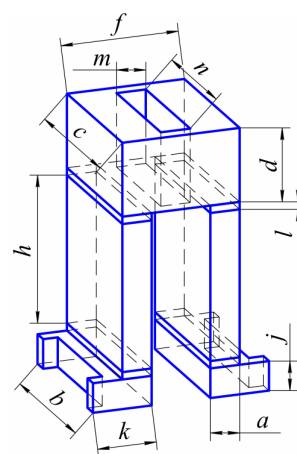
Heat carrier flow rate at thermoelement inlet was assumed equal to 0.1 mm/s, 0.5 mm/s, 1 mm/s, 2 mm/s, 3 mm/s, 4 mm/s and 5 mm/s. With each rate value the supply voltage assumed the values: 0.02 V, 0.04 V, 0.06 V, 0.08 V, 0.10 V, 0.12 V, 0.14 V, 0.16 V and 0.18 V. Coefficient of heat exchange between water and thermoelement α_T in the Newton-Richmann law was assumed equal to 1000 W/(m^2·K).

For the above parameters the following thermoelement characteristics were determined: the values of electric current I, A; flow rate G, m^3/s; outlet liquid temperature t, °C; thermoelement cold junction temperatures T, °C; temperature difference of liquid Δt, °C and thermoelement ΔT, °C; power W, W; cooling capacity Q_c, W; coefficient of performance ε.

From the results of computer calculation the following energy characteristics were obtained: cooling capacity, coefficient of performance (Fig. 3 *a*) and temperature difference on the water and thermoelement (Fig. 3 *b*) depending on thermoelement voltage and different water flow rate.
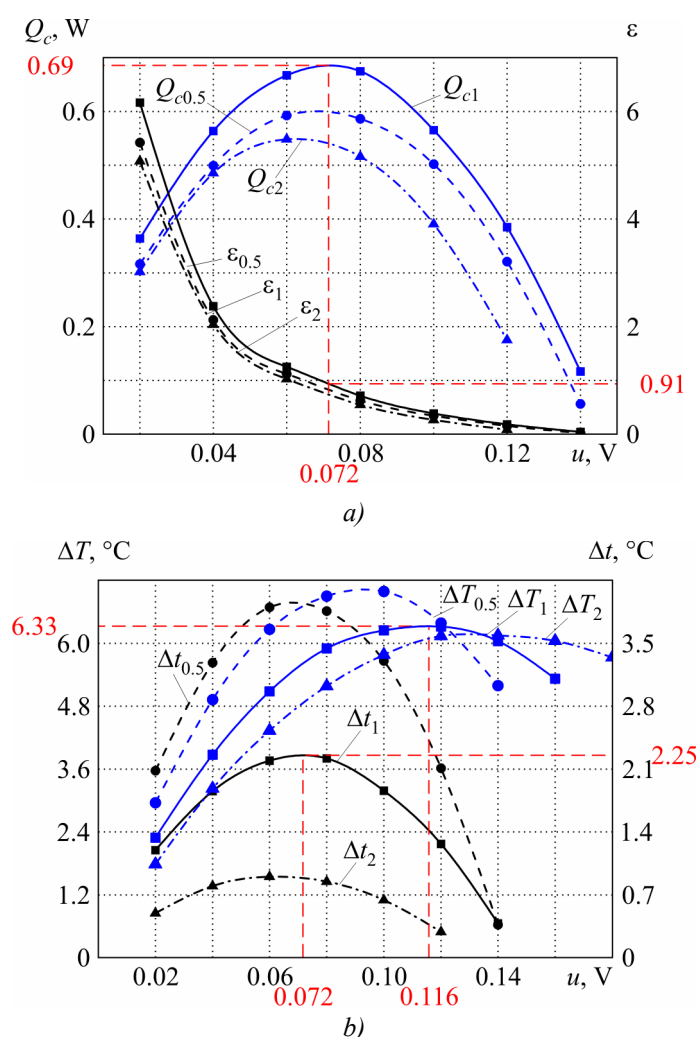

Fig. 3. Cooling capacity, coefficient of performance (a) and temperature difference of liquid and thermoelement (b) versus voltage for different rates: $Q_{c0.5}$, Q_{c1}, Q_{c2} is cooling capacity at liquid rate 0.5 mm/s, 1 mm/s, 2 mm/s, respectively; $\varepsilon_{0.5}$, ε_1, ε_2 is coefficient of performance at liquid rate 0.5 mm/s, 1 mm/s, 2 mm/s, respectively; $\Delta T_{0.5}$, ΔT_1, ΔT_2 is thermoelement temperature difference, $\Delta t_{0.5}$, Δt_1, Δt_2 is liquid temperature difference at the rate of 0.5 mm/s, 1 mm/s, 2 mm/s.

It is seen that maximum cooling capacity value falls on the rate $\upsilon = 1$ mm/s and makes $Q_c = 0.68$ W at the voltage of $u = 0.07$ V, and energy conversion at maximum cooling capacity occurs

with a thermodynamic efficiency $\varepsilon = 0.91$. Temperature difference on the thermoelement is $\Delta T = 6.3\ °C$ at the voltage of $u = 0.12\ V$, and temperature difference on the liquid $\Delta t = 2.25\ °C$.

To specify the value of optimal rate, the rate dependence of maximum cooling capacity with the optimal voltage has been constructed (Fig. 4). The same figure shows the dependence of temperature difference on the liquid obtained under these conditions.
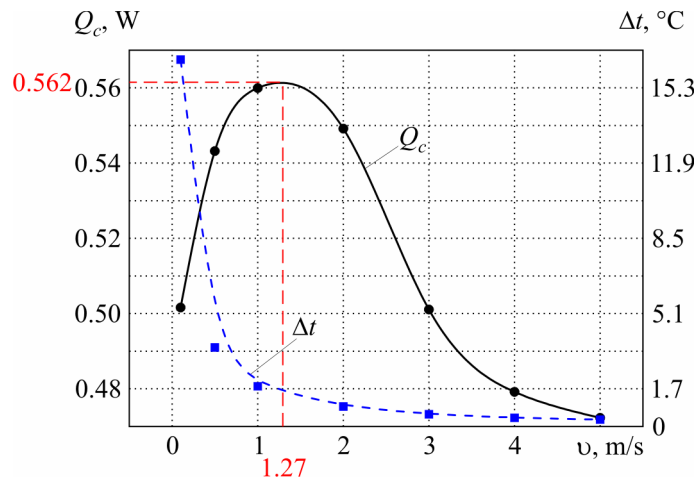

Fig. 4. Maximum cooling capacity and temperature difference
of liquid versus the rate.

It is seen that maximum cooling capacity value is achieved at the rate of $\upsilon = 1.27\ mm/s$. Temperature difference on the liquid increases with the rate decrease, which provides for a greater water cooling depth. A greater cooling depth calls for a lower water delivery rate, however, cooling capacity in this case is reduced. The existence of a rational range of water feed rate values determined by thermoelement operating mode is evident.

The distribution of temperature field in thermoelement and liquid at thermoelement voltage $u = 0.06\ V$ and optimal water rate at channel inlet $\upsilon = 1.27\ mm/s$ is given in Fig. 5 *a*. The distribution of rate field under these conditions is represented in Fig. 5 *b*.

In Fig. 5 *a* it is seen that the medium part of legs is overheated due to the Joule-Lenz heat release and heat input from the liquid. However, in the interconnect area the effect of Peltier heat is greater, which provides for water cooling. From Fig. 5 *b* it is seen that maximum rate is achieved with the lowest channel section.
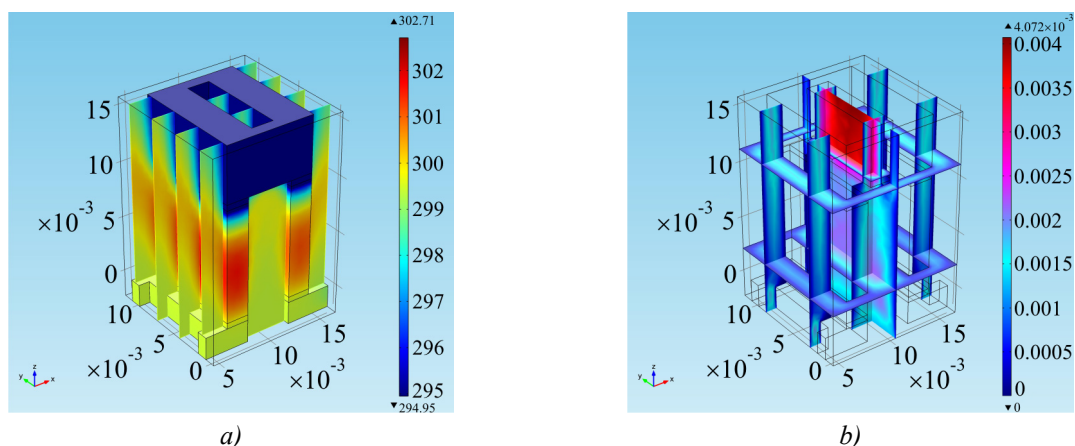

a)   *b)*

Fig. 5. Temperature distributions in the thermoelement and liquid (a)
and rate field distribution in the liquid (b).

Fig. 6 gives the dependences of the energy characteristics of liquid permeable thermoelement with the optimal liquid rate at channel inlet on thermoelement voltage.
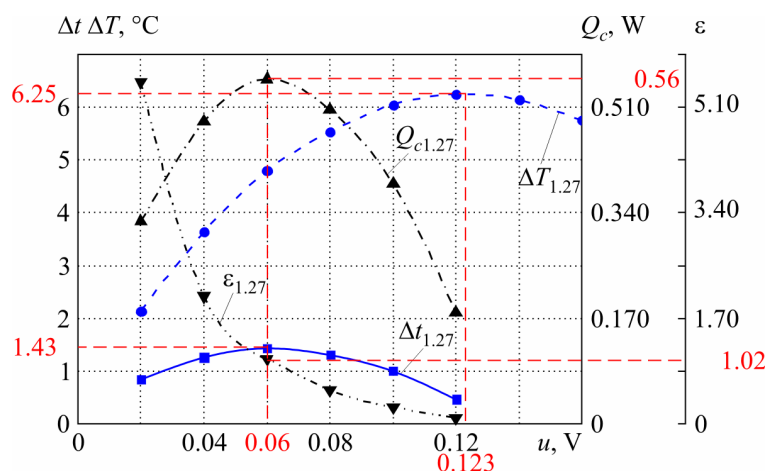

Fig. 6. Maximum cooling capacity Q_c, coefficient of performance ε, liquid temperature difference Δt, thermoelement ΔT versus voltage for the optimal rate.

It is evident from the figure that maximum value of cooling capacity Q_c = 0.56 W is achieved at the voltage of u = 0.06 V, and energy conversion in maximum cooling capacity mode occurs with thermodynamic efficiency ε = 1.023.

Maximum temperature difference value of thermoelement is equal to ΔT = 6.25 °C at the voltage of u = 0.12 V, and of liquid – Δt = 1.43 °C at the voltage of u = 0.06 V.

A similar computer model for the air thermoelement in cooling mode was developed. The specific feature of this model of permeable air thermoelement is that heat carrier properties are replaced by gas-air thermophysical properties. The heat-exchange coefficient at the water-air interface in the Newton-Richmann law is at a level of 100 W/(m²·K). The air rate at channel inlet was assumed equal to υ = 0.4 m/s. According to experimental investigations given in [6], this rate is optimal for the above geometry of thermoelement legs.

The distribution of temperature field in the thermoelement and in the air with the air rate at channel inlet υ = 0.4 m/s and thermoelement voltage u = 0.08 V is given in Fig. 7 *a*; the distribution of rate field in the air under these conditions is shown in Fig 7 *b*.
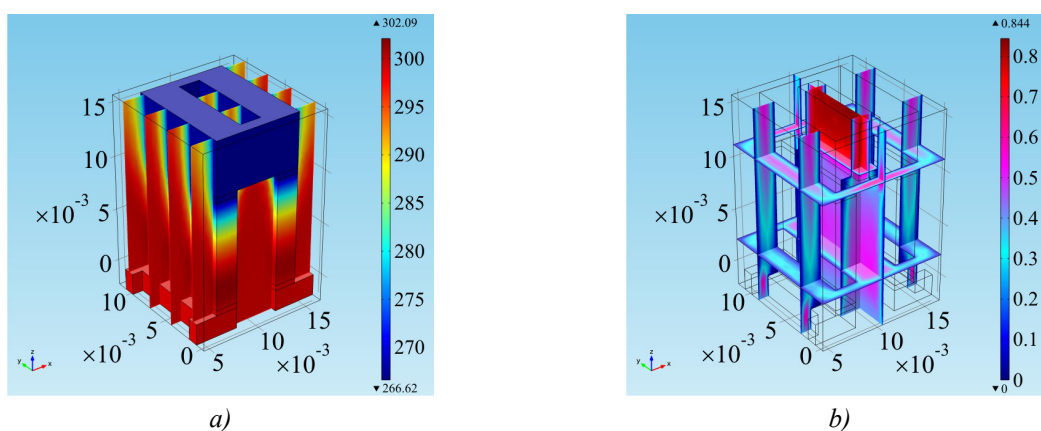

a)   *b)*

Fig. 7. Temperature field distribution in the thermoelement and in the air (a)
and rate field distribution in the air (b).

From Fig. 7 *a* it is seen that leg overheat due to the Joule-Lenz effect and thermal flux from the air is considerably less than in the liquid permeable thermoelement. Thus, one can make a conclusion

on the effect of thermophysical properties of liquid or gas heat carrier on the temperature field. The Peltier heat absorbed in the near-contact area prevails over heating and provides for cooling. From Fig. 7 *b* it is seen that the maximum rate is achieved with the smallest channel section which is similar to rate field distribution for water.

Fig. 8 shows voltage dependences of the energy parameters of the air thermoelement for the air rate at channel inlet $\upsilon = 0.4$ m/s.

From Fig. 8 it is seen that maximum cooling capacity value of the air permeable thermoelement $Q_c = 0.42$ W is achieved at the voltage of $u = 0.086$ V, and energy conversion with maximum cooling capacity occurs with the efficiency of $\varepsilon = 0.41$. Maximum temperature difference value of the air permeable thermoelement is equal to $\Delta T = 35.7\,°C$ at the voltage of $u = 0.11$ V, and of the liquid – $\Delta t = 11.44\,°C$ at the voltage of $u = 0.086$ V.
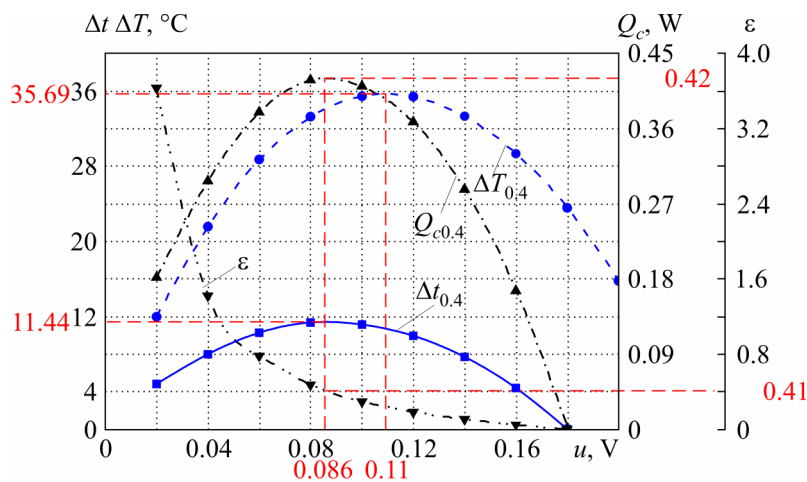

Fig. 8. Maximum cooling capacity Q_c, coefficient of performance ε, air temperature difference Δt, thermoelement temperature difference ΔT for the optimal rate versus voltage.

Based on the obtained results of calculation of permeable thermoelement for cooling liquid and gas flows in a three-dimensional case under optimal conditions, comparative dependences of cooling capacity and coefficient of performance have been constructed that are given in Fig. 9.
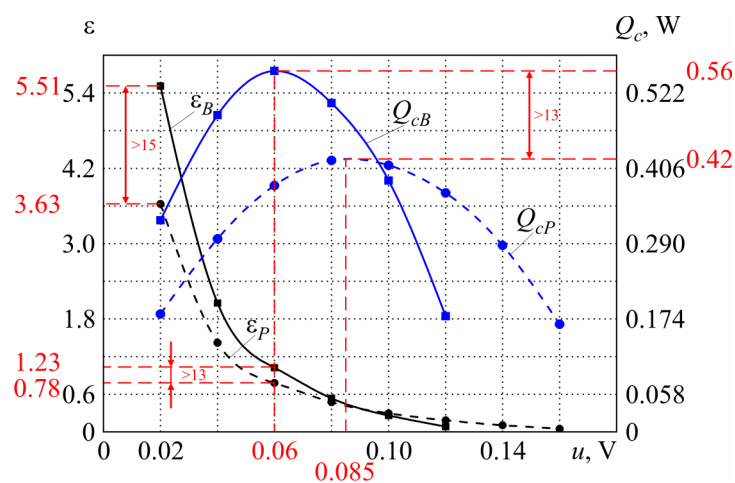

Fig. 9. Comparative dependence of cooling capacity Q_c, coefficient of performance ε for the liquid (index B) and the air (index P) on thermoelement voltage under optimal conditions.

From the above dependences it is seen that maximum cooling capacity value of the liquid permeable thermoelement $Q_{cB} = 0.56$ W is achieved at lower thermoelement voltage $u = 0.06$ V than

that of the air one – $Q_{cP} = 0.42$ W at a voltage of $u = 0.086$ V. In so doing, cooling capacity of the liquid thermoelement is higher than that of the air one by a factor of 1.3. Coefficient of performance of the liquid thermoelement at a voltage of $u = 0.02$ V exceeds that of the air thermoelement by a factor of 1.5, and at a voltage of $u = 0.06$ V – by a factor of 1.3.

Thus, there are optimal ranges of voltage values where the energy capabilities of permeable thermoelement for water cooling are superior to energy characteristics of thermoelement for air cooling. Therefore, there is a need in multi-parameter optimization of structural and thermophysical parameters of permeable thermoelement that will make it possible to determine maximum thermodynamic characteristics.

Conclusions

1. A 3*D* model of permeable thermoelement for cooling liquid and gas flows has been elaborated in the Comsol Multiphysics package of applied computer programs.
2. The distributions of temperatures in material of thermoelement legs and heat carrier, potentials in thermoelement, liquid rates and the energy characteristics of permeable thermoelement of materials based on *Bi-Te-Se-Sb* have been determined.
3. The effect of heat carrier pumping rate and thermoelement supply voltage on temperature difference and energy conversion characteristics has been investigated. The optimal values of water feed rate at channel inlets and potential difference on thermoelement whereby maximum cooling capacity is realized on liquid and air cooling have been determined.
4. Comparison of research results has shown the presence of such voltage range on thermoelement whereby the liquid permeable thermoelement outperforms the air one by a factor of 1.3 to 1.5.

References

1. L.I. Anatychuk, *Thermoelements and Thermoelectric Devices: Handbook* (Kyiv: Naukova Dumka, 1979), 768 p.
2. L.I. Anatychuk, *Physics of Thermoelectricity [Thermoelectricity, V. 1]* (Chernivtsi, 1998), 388 p.
3. G.J. Snyder, E.S. Toberer, Complex Thermoelectric Materials, *Nature Materials* **7**, 105 – 114 (2008).
4. L.I. Anatychuk, Current Status and Some Prospects of Thermoelectricity, *J. Thermoelectricity* **2,** 7 – 20 (2007).
5. L.I. Anatychuk, L.N. Vikhor, R.G. Cherkez, Optimal Control of the Inhomogeneity of Semiconductor Material for Permeable Cooling Thermoelements, *J. Thermoelectricity* **3**, 45 – 55 (2000).
6. L.I. Anatychuk, R.G. Cherkez, D.D. Demyanyuk, and N.R. Bukharayeva, Research on the Energy Characteristics of Permeable Plane Thermoelement, *J. Thermoelectricity* **2**, 84 – 88 (2012).
7. L.I. Anatychuk, V.A. Semenyuk, *Optimal Control of the Properties of Thermoelectric Materials and Devices* (Chernivtsi: Prut, 1992), 264 p.
8. I.M. Kadenko, O.M. Kharitovov, R.V. Yermolenko, *The Basics of Thermal Hydraulics of Nuclear Energy Installations* (Kyiv: Publishing and Printing Centre "Kyiv University", 2010), 320 p.
9. D.I. Okhrimenko, *The Use of COMSOL Multiphysics 3.4 Package for Solving Hydrodynamics and Heat Exchange Problems in Chemical Technology* [Yearly Project] (Donetsk, 2009), 64 p.
10. G.V. Biryullin, *Thermophysical Calculations in Finite-Element Package COMSOL/FEMLAB: Manual* (Saint-Petersburg: The National Research University ITMO, 2006), 78 p.
11. http://www.coml.com.